

Article

GPS-Derived Fault Coupling of the Longmenshan Fault Associated with the 2008 Mw Wenchuan 7.9 Earthquake and Its Tectonic Implications

Yanchuan Li ¹, Guohong Zhang ¹, Xinjian Shan ^{1,*}, Yunhua Liu ¹, Yanqiang Wu ²,
Hongbao Liang ², Chunyan Qu ¹ and Xiaogang Song ¹

¹ State Key Laboratory of Earthquake Dynamics, Institute of Geology, China Earthquake Administration, Beijing 100029, China; yanliupcc@gmail.com (Y.L.); zhanggh@ies.ac.cn (G.Z.); liuyunhua@ies.ac.cn (Y.L.); dqyquchy@163.com (C.Q.); sxghohai@163.com (X.S.)

² First Crust Deformation Monitoring and Application Center, China Earthquake Administration, Tianjin 300180, China; chdqyw@126.com (Y.W.); lhb131421@126.com (H.L.)

* Correspondence: xjshan@ies.ac.cn; Tel.: +86-010-6200-9134

Received: 9 March 2018; Accepted: 12 May 2018; Published: 15 May 2018



Abstract: Investigating relationships between temporally- and spatially-related continental earthquakes is important for a better understanding of the crustal deformation, the mechanism of earthquake nucleation and occurrence, and the triggering effect between earthquakes. Here we utilize Global Positioning System (GPS) velocities before and after the 2008 Mw 7.9 Wenchuan earthquake to invert the fault coupling of the Longmenshan Fault (LMSF) and investigate the impact of the 2008 Mw 7.9 Wenchuan earthquake on the 2013 Mw 6.6 Lushan earthquake. The results indicate that, before the 2008 Mw 7.9 Wenchuan earthquake, fault segments were strongly coupled and locked at a depth of ~18 km along the central and northern LMSF. The seismic gap between the two earthquake rupture zones was only locked at a depth < 5 km. The southern LMSF was coupled at a depth of ~10 km. However, regions around the hypocenter of the 2013 Mw 6.6 Lushan earthquake were not coupled, with an average coupling coefficient ~0.3. After the 2008 Mw 7.9 Wenchuan earthquake, the central and northern LMSF, including part of the seismic gap, were decoupled, with an average coupling coefficient smaller than 0.2. The southern LMSF, however, was coupled to ~20 km depth. Regions around the hypocenter of the 2013 Mw 6.6 Lushan earthquake were also coupled. Moreover, by interpreting changes of the GPS velocities before and after the 2008 Mw 7.9 Wenchuan earthquake, we find that the upper crust of the eastern Tibet (i.e., the Bayan Har block), which was driven by the postseismic relaxation of the 2008 Mw 7.9 Wenchuan earthquake, thrust at an accelerating pace to the Sichuan block and result in enhanced compression and shear stress on the LMSF. Consequently, downdip coupling of the fault, together with the rapid accumulation of the elastic strain, lead to the occurrence of the 2013 Mw 6.6 Lushan earthquake. Finally, the quantity analysis on the seismic moment accumulated and released along the southern LMSF show that the 2013 Mw 6.6 Lushan earthquake should be defined as a “delayed” aftershock of the 2008 Mw 7.9 Wenchuan earthquake. The seismic risk is low along the seismic gap, but high on the unruptured southwesternmost area of the 2013 Mw 6.6 Lushan earthquake.

Keywords: the Longmenshan fault zone; the 2013 Mw 6.6 Lushan earthquake; the 2008 Mw 7.9 Wenchuan earthquake; earthquake triggering; fault coupling

1. Introduction

The Longmenshan Fault (LMSF) zone, known as a major thrusting boundary structure, is located at the eastern margin of the Tibetan Plateau, which separates the plateau and the stable South China

block [1,2] (Figure 1). The LMSF zone bears particular significance for understanding the uplifting mechanism of the Tibetan Plateau, since it is closely related to the formation of the Longmenshan Mountains, which is controlled by the eastern extrusion of the Tibetan Plateau (e.g., [3,4]). In addition, the LMSF zone controls the crustal deformation and seismicity at the Longmenshan region [5–7]. Commonly, intercontinental active tectonic faults are characterized by depth-dependent crustal behaviors, with repeated earthquake ruptures and interseismic coupling in the upper/middle crust, and quasi-stable aseismic creep in the deeper substrate [8]. Thus, investigating the fault coupling of the LMSF and its variation along depth is of great significance for understanding the seismic activities and crustal deformation of the Eastern Tibetan Plateau.

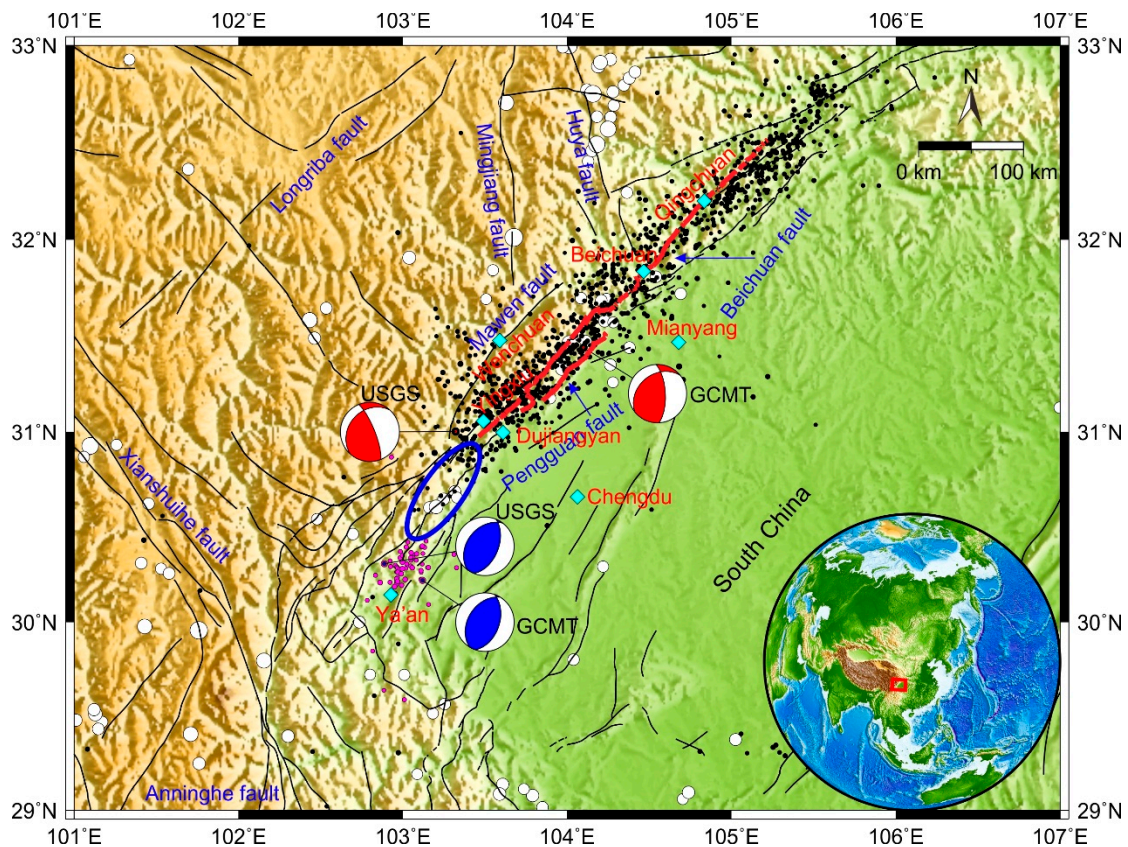


Figure 1. Regional tectonic map of the Longmen Shan region. White dots represent background seismicity before 2008 (1930–2008, USGS—U.S. Geological Survey). Black dots are the aftershocks of the 2008 Mw 7.9 Wenchuan earthquake (until April 2013, USGS). Magenta dots show aftershocks of the 2013 Mw 6.6 Lushan earthquake (till March 2016, USGS). The focal mechanisms shown in red and blue beach balls, which come from the USGS and Global CMT, correspond to the 2008 Mw 7.9 Wenchuan earthquake and the 2013 Mw 6.6 Lushan earthquake, respectively. Black and red lines indicate regional faults and surface traces of co-seismic rupture of the Wenchuan earthquake [2]. The blue oval shows the approximate location of the “seismic gap” caused by the 2008 Mw 7.9 Wenchuan earthquake and the 2013 Mw 6.6 Lushan earthquake. The central and northern LMSF are located to the northeast of the gap, and the southern LMSF to the southwest. Green diamonds indicate the main cities or residential areas. Image overlain on the 30 m Shuttle Radar Topography Mission Digital Elevation Database (SRTM DEM). The red rectangle in the inset shows the study area.

On 12 May 2008, the devastating Mw 7.9 Wenchuan earthquake ruptured the LMSF and generated a 240-km-long surface rupture along the Beichuan Fault and a 72-km-long surface rupture along the Pengguan Fault [2]. The earthquake propagated unilaterally to the northeast, leaving the southern segments of the LMSF (hereafter referred to as the southern LMSF) unbroken [9,10] (Figure 1).

In addition, the southern LMSF accommodated few aftershocks [11]. On 20 April 2013, the Mw 6.6 Lushan earthquake ruptured the southern LMSF and filled part of the rupture deficit along the southern LMSF [12]. However, an approximately 60-km-long segment between the rupture zones of the two earthquakes remain unruptured, forming an apparent “seismic gap” [13] (Figure 1). It remains debated that the seismic risk of the 60-km-long seismic gap. Chen et al. [12] and Liu et al. [14,15] suggested that the likelihood of future earthquakes is very high due to the co-seismic coulomb stress loading from the 2008 Mw 7.9 Wenchuan and 2013 Mw 6.6 Lushan earthquakes. Li et al. [16] and Dong et al. [13], in contrast, claimed that the seismic gap is not particularly stressed-up and, thus, the risk for future earthquakes is not especially high. In addition, the 2008 Mw 7.9 Wenchuan and the 2013 Mw 6.6 Lushan events are close, spatially, and have a short time interval of only five years. Thus, a large number of studies have focused on their relationship and have obtained discrepant results (e.g., [12,14,17–19]). For instance, there are debates about whether the 2013 Mw 6.6 Lushan earthquake was an aftershock of the 2008 Mw 7.9 Wenchuan earthquake (e.g., [12,14,17,19,20]). Moreover, previous studies indicated that both the co-seismic rupture and postseismic relaxation due to the 2008 event may have increased the stress level on the southern LMSF, which triggered the 2013 event (e.g., [14,18,21]). However, such studies have not considered the interseismic fault coupling characteristics [22].

In view of the aforementioned issues and debates, we use the horizontal GPS velocities to invert the fault coupling of the LMSF before and after the 2008 Mw 7.9 Wenchuan earthquake. We first introduce the GPS data, its processing strategies, and our modeling strategies. Then the inversion results of the fault coupling of the LMSF are analyzed, in attempting to investigate the possible impact of the 2008 Mw 7.9 Wenchuan earthquake on the nucleation and occurrence of the 2013 Mw 6.6 Lushan earthquake. Relationships between the 2008 Mw 7.9 Wenchuan earthquake and the 2013 Mw 6.6 Lushan earthquake are then discussed, as well as the seismic hazard along the “seismic gap”.

2. GPS Data and Modeling Strategies

2.1. GPS Data and Its Processing

GPS data collected during 1999–2007 and 2009–2013 were used to invert the fault coupling of the LMSF before and after the 2008 Mw 7.9 Wenchuan earthquake, respectively. As for the secular velocity solutions before the 2008 Mw 7.9 Wenchuan earthquake, we used 547 GPS stations located in the study area [23], with an average error of 1.6 mm/a (Figure 2). We selected the GPS observations between April 2009 and April 2013 (before the 2013 Mw 6.6 Lushan earthquake), which are from two sources: (1) the Sichuan Global Navigation Satellite System (GNSS) Network of the Sichuan Earthquake Bureau, which contains 37 continuous GNSS sites, with 14 sites conducted from January 2004 to April 2013 and 23 sites from August 2010 to April 2013; and (2) the Crustal Movement Observation Network of China (CMONOC), including 441 Campaign sites and 16 continues sites. Campaign sites were conducted in 2009, 2011, and 2013, respectively, lasting at least 72 h in each survey. The GAMIT/GLOBK 10.6 software [24,25] was used to process the regional GPS data. Raw pseudo-range and phase observations were first processed together with 36 globally-distributed International GNSS Service (IGS) stations to obtain daily loosely-constrained station coordinates and the satellite orbits parameters. The time series of each station were carefully checked to avoid outliers. The daily solutions were then transformed into the International Terrestrial Reference Frame (ITRF2008) by estimating seven transformation parameters (three orientation, three translation and one scale parameters) using the 36 globally-distributed IGS stations. Finally, the velocities were transformed into a Eurasia-fixed reference frame using the Euler vector for Eurasia with respect to the ITRF2008, with an averaged error of 0.7 mm/a [26] (Figure 2).

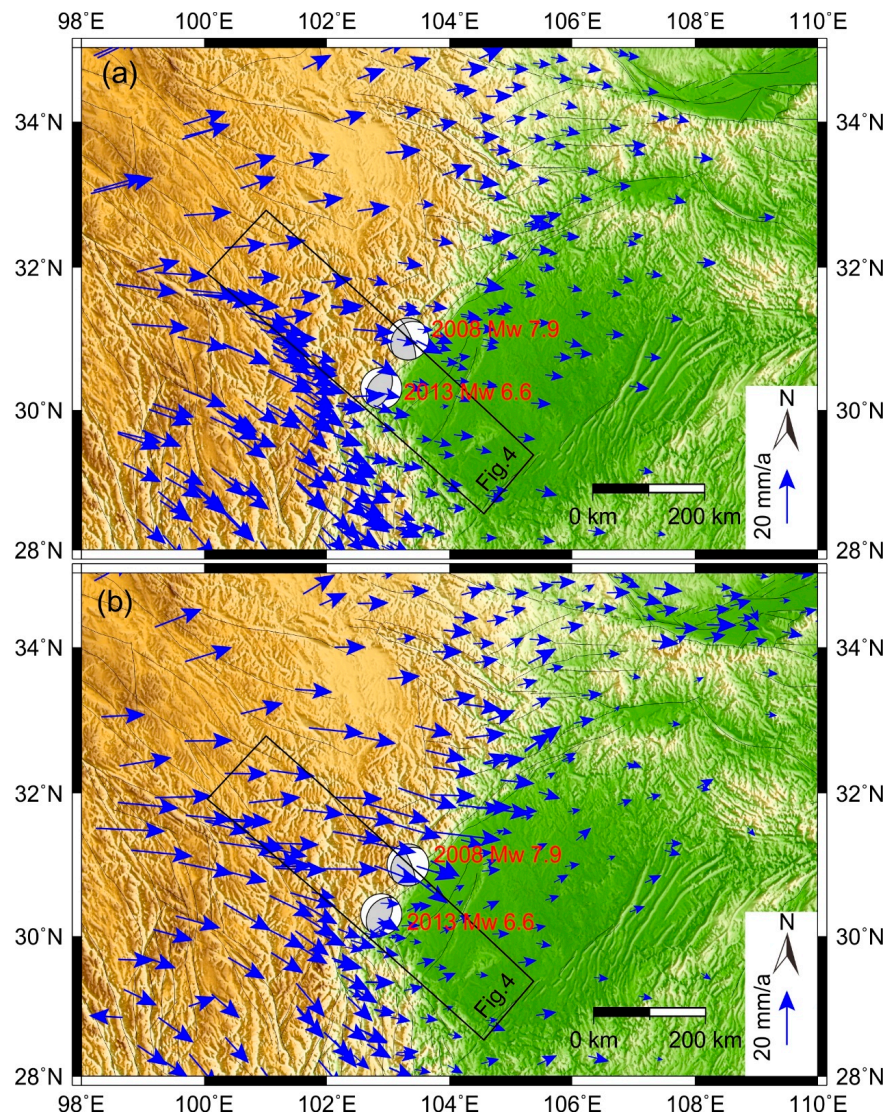


Figure 2. Measured motion of GPS sites in the Eastern Tibetan Plateau before (a) [23] and after (b) the 2008 Mw 7.9 Wenchuan earthquake. GPS velocity vectors are relative to the Eurasia fixed frame. For clarity, the error ellipses are not shown. Grey lines indicate regional faults. The black rectangle marks the location of the cross-fault profile in Figure 4i.

Note that the GPS measurements before the 2008 Mw 7.9 Wenchuan earthquake are the secular interseismic velocities of the Tibetan Plateau relative to the stable Eurasia reference frame, whereas the solutions after the 2008 event include both interseismic velocities and transient postseismic deformation, the latter of which matters for our interpretation of the relationship between the 2008 Mw 7.9 Wenchuan earthquake and the 2013 Mw 6.6 Lushan earthquake. GPS time series show rapid decay following the 2008 Mw 7.9 Wenchuan earthquake, lasting for about nine months (by March 2009), which have been confirmed by Rui et al. [23]. As a result, instead of solving for the postseismic deformation of each GPS site by fitting the position time series, we estimate their linear velocities, which are treated as the average crustal deformation rate of the Eastern Tibetan Plateau in the period between the two concerned earthquakes. However, we must pay attention that this kind of linear fitting is not a strictly secular interseismic velocity solution, as GPS sites' velocities are affected postseismic transients. We obtained 95% of the residuals smaller than 3.2 mm after removing the linear trend (Figure S1). To separate signals related to the postseismic deformation of the 2008 Mw 7.9 Wenchuan earthquake, we subtracted the GPS velocity before the earthquake from that after the earthquake.

The premise of the simple practice is to assume that the crustal movements do not change over several earthquake cycles [27], and the changes of the crustal movement after an earthquake is related to postseismic transients. Other discrepancies affecting the comparison of the two velocity solutions include different processing strategies in data trade-off, frame choices, station partition, and a priori constraint [28]. Fortunately, there are 134 co-located sites in both datasets, which are at least 500 km away from the epicenter of the 2008 Mw 7.9 Wenchuan earthquake. We first solved for the Euler vector between the two solutions by minimizing the velocity residuals within common sites [28]. Then the velocity solution after the 2008 Mw 7.9 Wenchuan earthquake was translated into the reference frame of the solution before the event.

2.2. Modeling Strategies

We use the block modeling approach to estimate the block rotations, permanent strain within blocks, block-bounding fault slip rates, and fault coupling based on the GPS velocities data before and after the 2008 Mw 7.9 Wenchuan earthquake [29–31]. The process is implemented by the *TDEFNODE* package [30]. In this approach, the spatial variability of fault coupling is defined by the parameter ϕ (the coupling coefficient) [32]. If $\phi = 0$, the fault is fully creeping or decoupled at a long-term slip rate. If $\phi = 1$, the fault is fully coupled. To apply the block modeling approach to the crustal deformation after the 2008 Mw 7.9 Wenchuan earthquake, two prerequisites should be fulfilled—the movement and rotation of the upper crust are driven by the lower crust, and the upper crust is considered elastic even after the earthquake. The first prerequisite has long been proved, especially in the Eastern Tibetan Plateau (e.g., [33]). The upper crust is elastic after the 2008 Mw 7.9 Wenchuan earthquake is also reasonable, as the postseismic deformation derived from InSAR shows the viscoelastic lower crust below 45 km [34].

We divided the Eastern Tibetan Plateau into six blocks, namely, the South China block (SC), the Longmen Shan block (LM), the North Yunnan block (NY), the East Yunnan (EY), the Bayan Har block (BY), and the Lanzhou block (LZ) (Figure S2) [35]. Apart from the SC block, all the blocks are modeled to be elastic, implying that the three components of strain rate will be inverted to account for block internal deformation. We adopt the fault geometry along the central and northern LMSF of Shen et al. [6]. We model the southern LMSF to be listric in shape, with near surface fault dip angles decreasing from 40° to 24° at a depth of 30 km [36–38] (Figure S3). We discretize the fault model into many sub-faults, with an average 50 km along the strike and depth-dependent sampling along the downdip, which include 0.1, 4, 8, 12, 16, 20, and 30 km at depth. We solve ϕ for each sub-fault, which is further divided into $8 \text{ km} \times 4 \text{ km}$ patches along the strike and downdip and interpolated by the bilinear method (Figure S3). A smoothing factor of 1.0 on the ϕ values along the strike is imposed, that is, the variation in ϕ values per degree of distance ($\sim 111 \text{ km}$) cannot be greater than 1.0. To account for the crustal deformation induced by surrounding coupled faults, such as the Xianshuihe fault and the Longriba fault, we estimate the average fault locking depth (from 0.1 km to 35 km) using a grid search method. The minimum GPS velocity residual model shows an average fault locking depth of 22 km for the Eastern Tibetan Plateau, which is then set as the tight constraint during our inversions. Similar works (e.g., [36–42]) contributed to our understanding of the fault coupling along the LMSF, and here we included more GPS stations after the 2008 Mw 7.9 Wenchuan earthquake, which provide a better constraint for the inversions. We focused on the seismic gap between the two earthquake rupture zones, and the quantitative relationship between the 2008 Mw 7.9 Wenchuan earthquake and the 2013 Mw 6.6 Lushan earthquake. Additionally, we investigate the impact of the postseismic deformation of the 2008 Mw 7.9 Wenchuan earthquake on the 2013 Mw 6.6 Lushan earthquake. We also need to explain that similar work [31] argued that the deformation parameters, such as fault coupling and the slip rate of the faults, are largely insensitive to the block division. Using our best-fitting model, we obtained normalized root mean squares (NRMS) of 1.9 mm/a and 2.1 mm/a for the inversion of the GPS velocities before and after the 2008 Mw 7.9 Wenchuan earthquake, respectively, indicating a reasonable consistency between observations and the model. In addition, a resolution test shows

the resolving ability of the GPS data to the fault-coupling inversion. The modeling residuals are satisfactory, which are given Figure S4.

3. Fault Coupling of the Longmenshan Fault before and after the 2008 Mw 7.9 Wenchuan Earthquake

The inverted fault coupling of the LMSF pre-2008 and post-2008 is shown in Figure 3. Before the 2008 Mw 7.9 Wenchuan earthquake, the central and the northern LMSF were strongly coupled with the maximum fault locking depth of ~18 km, and the average fault coupling coefficient larger than 0.9 at the depth of 0–20 km (Figure 3a). The co-seismic rupture area of the 2008 Mw 7.9 Wenchuan earthquake overlaps the strongly-coupled segments of the central and northern LMSF, with 83% of the 2008 Mw 7.9 Wenchuan seismic moment released in the fully-coupled LMSF. Fault coupling around the hypocenter region changed rapidly from ~0.9 to ~0.3, indicating a large strain gradient. Large earthquakes tend to initiate in such transitional areas, such as the 2015 Nepal Mw 7.9 earthquake [28]. Our inversion result also indicates that, before the 2008 Mw 7.9 Wenchuan earthquake, the locking depth along the “seismic gap” segment between the 2008 Mw 7.9 Wenchuan and 2013 Mw 6.6 Lushan coseismic ruptures was less than 5 km and partially coupled at a depth of 5–20 km (Figure 3a). Along the southern LMSF, the strongly-coupled region was within a depth of ~10 km and the hypocenter of the 2013 Mw 6.6 Lushan earthquake located in a loosely-coupled region, with an average coupling coefficient ~0.3, indicating that the 2013 Mw 6.6 Lushan earthquake region has not been tightly coupled before the 2008 Mw 7.9 Wenchuan earthquake. Additionally, defining the shear modulus to be 30 GPa, the accumulated geodetic strain moment rate of the central and northern LMSF within a depth of 20 km is equivalent to $\sim 6.2 \times 10^{17}$ Nm/a. Assuming such a constant interseismic accumulation rate, depending on the released seismic moment (e.g., [6,10]), the recurrence interval for the 2008 Mw 7.9 Wenchuan earthquake vary between 1200 to 3200 years, which is roughly consistent with the paleoseismic result of at most 3000 years [43].

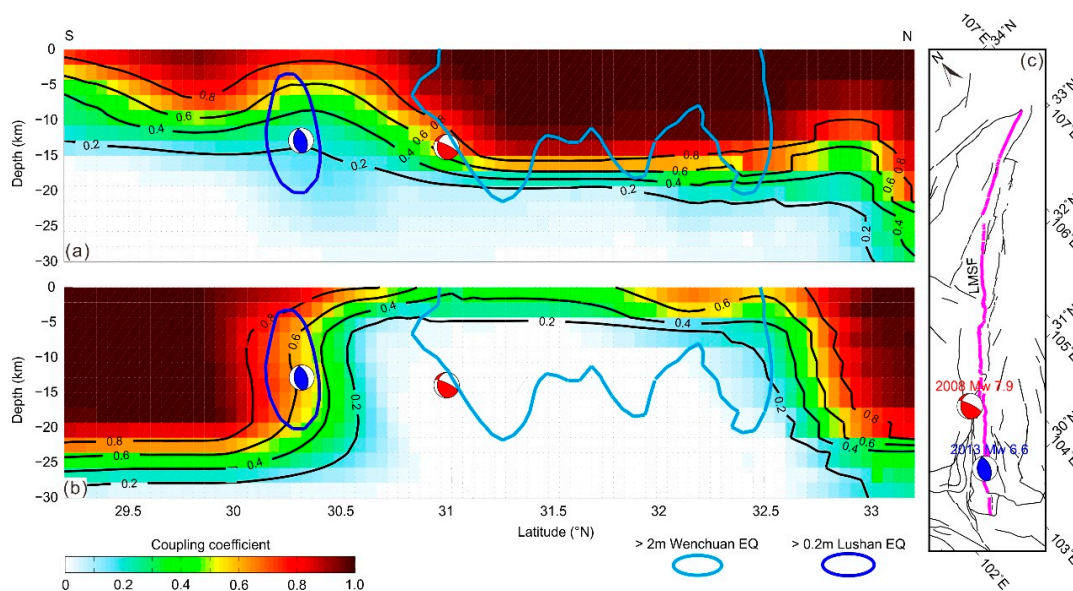


Figure 3. Fault coupling of the LMSF before (a) and after (b) the 2008 Mw 7.9 Wenchuan earthquake. White to reddish brown indicates the fault coupling coefficient. The red and blue focal mechanisms indicate epicentres of the 2008 Mw 7.9 Wenchuan earthquake and the 2013 Mw 6.6 Lushan earthquake respectively. The region of co-seismic slip > 2 m of the 2008 Mw 7.9 Wenchuan earthquake is outlined by the light blue line [6]. The region of co-seismic slip > 0.2 m of the 2013 Mw 6.6 Lushan earthquake is outlined by the blue line [37]. Black lines indicate fault coupling coefficient contours; and (c) oblique projection of regional faults in the Eastern Tibetan Plateau. The bold magenta line shows the surface trace of the LMSF in our model.

The inversion result based on GPS data measured after the 2008 Mw 7.9 Wenchuan earthquake indicate that the central and northern LMSF has been dramatically decoupled, with an average coupling coefficient smaller than 0.1 at depth of 5–20 km (Figure 3b), such as the case of the Andean megathrust after the 2010 Maule M 8.8 earthquake [27]. Our coupling model shows that the “seismic gap” segment has also been decoupled after the 2008 Mw 7.9 Wenchuan earthquake, with the average coupling coefficient reduced from 0.5 to 0.2 (Figure 3b). We also find that the average locking depth increases from ~5 km to ~25 km along the southern LMSF. Moreover, after the 2008 Mw 7.9 Wenchuan earthquake, the region accommodating the hypocenter of the 2013 Mw 6.6 Lushan earthquake has a coupling coefficient increases rapidly from 0.3 to 0.7, indicating an enhanced coupling effect. In addition, the co-seismic rupture of the 2013 Mw 6.6 Lushan earthquake coincides well with the coupled region along the southern LMSF (Figure 3b).

The comparison shows that, some strongly-coupled regions beneath and around the 2008 Mw 7.9 Wenchuan co-seismic rupture become almost fully decoupled after the 2008 event (Figure 3). Such sharp contrast of the fault coupling on the central and northern LMSF may indicate that the accumulated strain on the strongly coupled regions beneath the 2008 Mw 7.9 Wenchuan co-seismic rupture might have been released by aftershocks, afterslip and viscoelastic relaxation [34]. Also note that the 2008 Mw 7.9 Wenchuan earthquake ruptured only part of the northern LMSF and the northernmost segment is almost fully coupled, but with no co-seismic rupture. However, the inversion resolution on the northernmost segment is limited, thus, we leave the discussion in future studies.

During the inversion, we have tried different model settings. For example, the spacing fault nodes along strike and downdip directions were set as 20 km, 30 km, 40 km, 50 km, and 60 km. Such test inversion indicates that the variation of ϕ along the strike can be detected at a distance of 50 km (Figure S4), and that along downdip makes no difference to the data fitting (with the NRMS from 1.9 mm/a to 2.2 mm/a). Moreover, the statistical results of velocity residuals exhibit Gaussian distribution (Figure S2), indicating that the velocity data were well fitted (NRMS of 1.9 mm/a and 2.1 mm/a). In addition, GPS velocity residuals from the post-Wenchuan earthquake are larger than that derived from the pre-Wenchuan earthquake model, implying that the postseismic deformation might have some impacts on the GPS data fitting. However, as we mentioned in Section 2.1, the block approach is also effective for the crustal deformation modeling after the 2008 Mw 7.9 Wenchuan earthquake, which mainly focuses on the kinematics of the upper crust and deformation behaviors of block bounding faults (e.g., [30–32]).

4. Discussions

4.1. Unilateral Rupture Propagation of the 2008 Mw 7.9 Wenchuan Earthquake

The kinematic rupture process of the 2008 Mw 7.9 Wenchuan earthquake shows a unilateral propagation to the northeast (e.g., [2,9,10,44]), which was reported to be caused by the effect of the crustal material strength (e.g., [45–47]). Zhu and Yuan [47] simulated the dynamic spontaneous rupture process of the 2008 Mw 7.9 Wenchuan earthquake using a two-dimensional finite element method and concluded that the crustal material strength difference between the hanging wall and the footwall of the LMSF is a key factor leading to the unilateral propagation. Additionally, based on seismic tomography, Xu et al. [45] found a sharply-contrasting zone compared to the surroundings, with low V_p and V_s and high Poisson's ratio anomalies in the upper crust of the central LMSF region, which was interpreted to be associated with fluid-bearing ductile flow (weak and ductile crust) and act as a barrier for the 2008 Mw 7.9 Wenchuan co-seismic rupture. Our inversion results show that before the 2008 Mw 7.9 Wenchuan earthquake, the “seismic gap” segment in the central LMSF was fully coupled at a relatively shallow depth (<5 km) (Figure 3a), and only partially-coupled or creeping at the middle depth (5–20 km). Crusts of these two depths are thought to be difficult to accumulate enough strain energy for future big earthquakes. Additionally, fault coupling might be closely related to fault frictional strength and the state of fault stress (e.g., [8]). Thus, our fault coupling results

suggest that the unilateral propagation of the 2008 Mw 7.9 Wenchuan earthquake is due to the fault strength heterogeneity between the northern and central LMSF. Indeed, some studies have reported that the fault strength of the LMSF zone might be rather inhomogeneous, compared to the faults in subduction zones or continental strike-slip faults (e.g., [36]). Furthermore, the geometry between the thrust movement due to long-term tectonic loading and the variations of the strike may have caused different states of stress along the LMSF, which, we suggest, results in different initial stress before the occurrence of the 2008 Mw 7.9 Wenchuan earthquake, which has caused the unilateral propagation to the northeast [48].

4.2. Nucleation and Occurrence of the 2013 Mw 6.6 Lushan Earthquake

Most studies suggest that both the co-seismic and postseismic Coulomb stress changes caused by the 2008 Mw 7.9 Wenchuan earthquake have advanced the occurrence of the 2013 Mw 6.6 Lushan earthquake, though they considered only a specific receiver fault (e.g., [14,18,21]). Our inversion results show that the hypocenter region of the 2013 Mw 6.6 Lushan earthquake was only loosely coupled, with a coupling coefficient of 0.3, before the occurrence of the 2008 Mw 7.9 Wenchuan earthquake, indicating that the southern LMSF was in an elastic strain accumulation deficit state or viscoelastic creeping state. The segments, however, were strongly coupled, with a coupling coefficient of 0.7, after the 2008 event, which is essential for the nucleation of earthquakes (Figure 3b).

In order to explore the relationship between the two events, a $0.5^\circ \times 0.5^\circ$ interpolation was performed on the GPS velocity changes (the velocity after the 2008 Mw 7.9 Wenchuan earthquake minus the velocity before the earthquake) of the co-located sites. The interpolated velocities were then used to calculate the crustal rotation rates and principle strain rates. The GPS velocity changes may be driven by the postseismic deformation (e.g., viscoelastic relaxation of the lower crust) of the 2008 Mw 7.9 Wenchuan earthquake. Details of the calculation are given in the supplementary material. We find that the postseismic effect of the 2008 Mw 7.9 Wenchuan earthquake has caused the Eastern Tibetan Plateau to thrust eastward with an accelerating average rate of $\sim 6\text{--}9$ mm/a (Figures 4a–i and 5a), and enhanced the compressive strain on the southern LMSF (Figure 5b). The decoupling of the central and northern LMSF and the postseismic deformation after the 2008 Mw 7.9 Wenchuan earthquake have accelerated the fault coupling and elastic strain accumulation on the southern LMSF, which contribute to the occurrence of the 2013 Mw 6.6 Lushan earthquake. For a more intuitive interpretation, we simulated the effect of postseismic deformation on a fault. Results show that the postseismic deformation could enhance the compression and shear stress on the fault plane, and accelerate the downward coupling and accumulation of elastic strain on the fault plane (Figure 6). Some more detailed information is also provided in the supplementary material. Moreover, the Coulomb stress loading imposed by the 2008 Mw 7.9 Wenchuan earthquake may have advanced the 2013 Mw 6.6 Lushan earthquake (e.g., [18,21]). Therefore, we suggest that the 2013 Mw 6.6 Lushan earthquake is a triggered event, considering the accelerating elastic strain accumulation and the Coulomb stress loading.

4.3. Was the 2013 Mw 6.6 Lushan Earthquake an Aftershock of the 2008 Mw 7.9 Wenchuan Earthquake?

Aftershocks are events that typically begin immediately following the mainshock over the entire rupture area and its surroundings [49]. Concerning whether the 2013 Mw 6.6 Lushan earthquake should be defined as an aftershock of the 2008 Mw 7.9 Wenchuan earthquake, controversial conclusions have been reached since the occurrence of the 2013 Mw 6.6 Lushan earthquake (e.g., [17,18]). For instance, Xu et al. [17] reported that the 2008 Mw 7.9 Wenchuan and the 2013 Mw 6.6 Lushan earthquake are independent rupturing events concerning their differences in rupture process, seismogenic structures, and aftershock distributions. By analyzing seismic reflection profiles, Li et al. [14] also suggested that the 2013 Mw 6.6 Lushan earthquake should be an independent event. On the other hand, Zhu [19] stated that the Lushan event should be one of the aftershocks, and possibly the largest one, of the 2008 Mw 7.9 Wenchuan mainshock, based on the analysis the statistical properties of the Wenchuan-Lushan earthquake sequence using three established empirical laws on

aftershocks, i.e., the Gutenberg-Richter relation, modified Omori-Utsu law, and B ath’s law. In addition, Wang et al. [18] evaluated the Coulomb stress change caused by coseismic rupture and postseismic stress relaxation of the 2008 Mw 7.9 Wenchuan earthquake at the rupture zone of the 2013 Mw 6.6 Lushan earthquake, and compared it with the tectonic loading Coulomb stress on the fault since the 2008 Mw 7.9 Wenchuan earthquake. They concluded that the 2013 Mw 6.6 Lushan earthquake is at least 85% of a delayed aftershock of the 2008 Mw 7.9 Wenchuan earthquake.

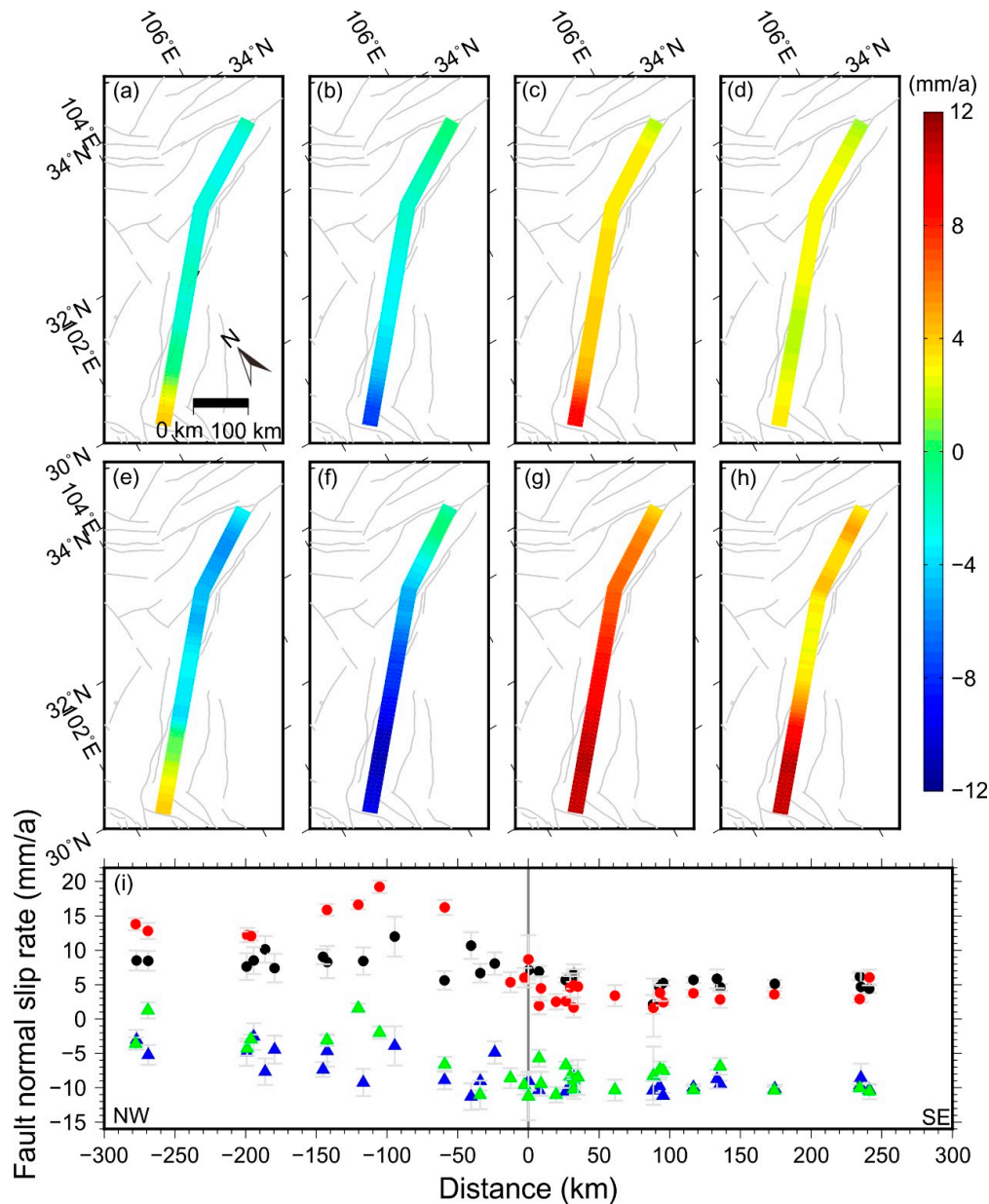


Figure 4. Statistics of the fault parallel slip rate (a,e); fault normal slip rate (b,f); total magnitude of slip rate (c,g); and the slip rate deficit (d,h) along the LMSF before (a–d) and after (e–h) the 2008 Mw 7.9 Wenchuan earthquake. Positive values indicate right-lateral or divergence; and (i) the GPS velocities across the southern LMSF. Black dots and red dots indicate fault-parallel velocity components before and after the 2008 Mw 7.9 Wenchuan earthquake. Green triangles and blue triangles represent fault-normal velocity components before and after the 2008 Mw 7.9 Wenchuan earthquake. Error bars are in 1- σ .

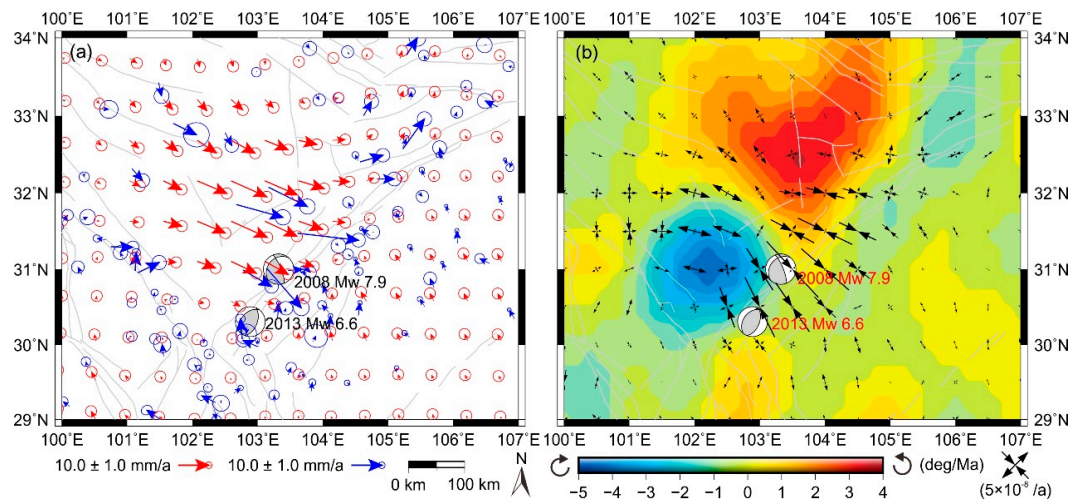


Figure 5. (a) The GPS velocity changes before and after the 2008 Mw 7.9 Wenchuan earthquake. Blue vectors indicate the crustal deformation after the 2008 Mw 7.9 Wenchuan earthquake, which are the difference between the 1999–2007 GPS velocities and the 2009–2013 GPS velocities. Error ellipses show the 95% confidence levels in 1- σ . Arrows in red indicate the interpolated velocity changes using the least squares collocation algorithm; and (b) the derived strain rate based on the interpolated postseismic deformation. The background colors indicate the crustal rotation rates derived from the GPS data, red indicates counterclockwise rotation and blue indicates clockwise rotation. Two arrows opposing each other indicate the extensional and compressional principal strain rates, respectively. Thin grey lines correspond to active faults. The focal mechanisms of the 2008 Mw 7.9 Wenchuan earthquake and the 2013 Mw 6.6 Lushan earthquake are also shown.

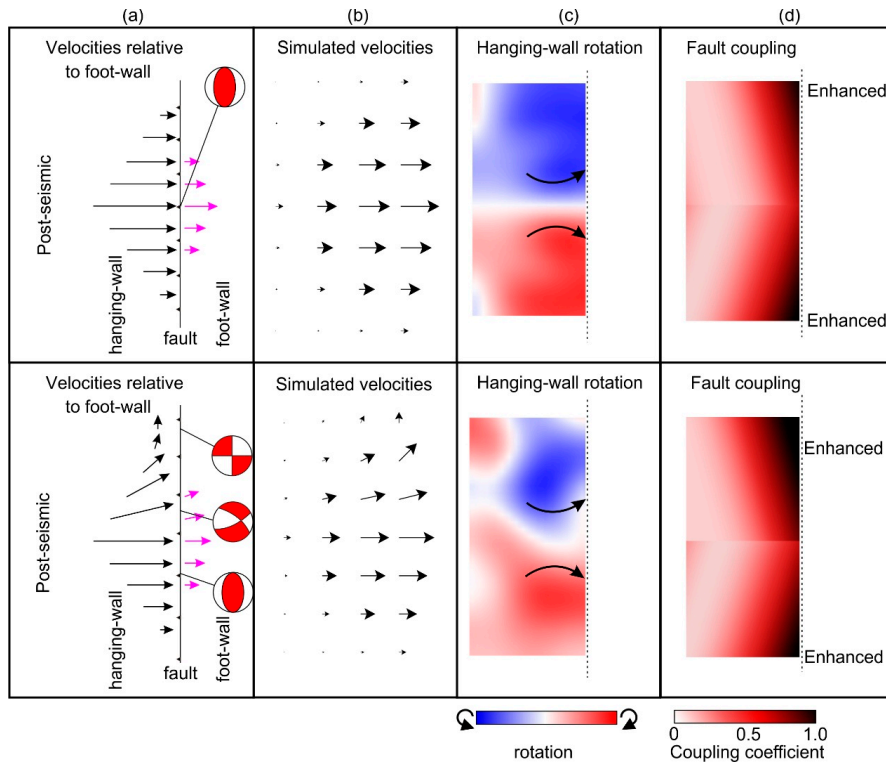


Figure 6. Sketch of the postseismic deformation model. (a) The assumed postseismic deformation and the corresponding kinematic characteristics of the fault; (b) the interpolated postseismic deformation velocity field by using the least-squares collocation method; (c) the derived crustal rotation rate of the hanging wall; and (d) the change of the fault coupling caused by the hanging wall rotation.

To investigate whether the 2013 Mw 6.6 Lushan earthquake should be defined as an aftershock of the 2008 Mw 7.9 Wenchuan earthquake, we summed the accumulated geodetic seismic moment rates on each patch along the southern LMSF and got 1.35×10^{18} Nm/a accumulation rate between 2008 and 2013. Assuming the rate to be constant over this period, the accumulated strain is equivalent to an Mw 6.5 earthquake (6.76×10^{18} Nm), accounting for 71% of the seismic moment released in the 2013 Mw 6.6 Lushan earthquake. The remaining 29% might accumulate on the fault plane interseismically, as indicated by the shallowly (<5 km), but coupled, results before the 2008 Mw 7.9 Wenchuan earthquake (Figure 3a). As stated by Savage and Prescott [50], fault begins to couple and accumulate elastic strain during the interseismic phase and releases the accumulated seismic moment during the co-seismic rupture, which is a traditional earthquake cycle. Although much of the seismic moment has been accumulated after the 2008 Mw 7.9 Wenchuan earthquake, the accumulated seismic moment is exactly the amount foreseen by an aftershock event e.g., [12], and the elastic strain buildup has been provided mainly by the mainshock. Also note that aftershocks are typically defined as events that begin immediately following the mainshock over the entire rupture area and its surroundings [49]. The time interval between the 2008 Mw 7.9 Wenchuan earthquake and the 2013 Mw 6.6 Lushan earthquake reaches five years. However, the temporal window of one seismic sequence is somehow arbitrary, no consensus has been reached so far. Therefore, under the existing framework of knowledge (e.g., empirical laws), we propose that the 2013 Mw 6.6 Lushan earthquake should be defined as a “delayed aftershock” of the 2008 Mw 7.9 Wenchuan earthquake. The inference is consistent with that proposed by Wang et al. [18], but we argue from different perspectives.

4.4. Seismic Hazard along the Southern LMSF

After the 2013 Mw 6.6 Lushan earthquake, there are controversies about the seismic hazard along the segment of the “seismic gap” and the southern LMSF. For example, Chen et al. [12] calculated the moment deficit along the unruptured segments of the LMSF between the 2008 Mw 7.9 Wenchuan and the 2013 Mw 6.6 Lushan rupture zones, and stated there is a high seismic risk on the “seismic gap”, which might be capable of generating an Mw 6.6 earthquake. Li et al. [20] and Liu et al. [14,15] also suggested that the unruptured segment is most likely to produce a large earthquake ($M \sim 7$) by interpreting results from 3D a numerical interseismic deformation simulation and co-seismic Coulomb stress calculation. On the other hand, both geologic trenches and seismic profiling suggest a low probability of a large earthquake along the gap in the near future [13,46], which is also supported by our fault-coupling model. Before the 2008 Mw 7.9 Wenchuan earthquake, the “seismic gap” segment along the southern LMSF was shallowly coupled (<5 km) (Figure 3a). Thus, viscoelastic creeping is expected at a deeper depth under the coupled region because of the low fault coupling coefficient (<0.4). The calculated geodetic moment accumulation rate on the fault plane (0–20 km) along the “seismic gap” is 1.35×10^{16} Nm/a, only accounted for 1% of the entire LMSF. After the 2008 Mw 7.9 Wenchuan earthquake, the fault plane along the “seismic gap” was completely decoupled (fault coupling coefficient ~ 0.3) (Figure 3b). Since the elastic strain cannot accumulate in the creeping fault plane (e.g., [30,32]), the decoupled “seismic gap” is not capable of accumulating elastic strain. Thus, we conclude that the seismic risk is not high at the unruptured segments along the LMSF between the 2008 Mw 7.9 Wenchuan and the 2013 Mw 6.6 Lushan rupture zones.

However, our fault-coupling results show that the southernmost LMSF is coupled ~ 20 km deep both before and after the 2008 Mw 7.9 Wenchuan earthquake. Assuming a time scale of 1000 years and a constant seismic moment deficit along the southern LMSF, the accumulated moment should be 2.96×10^{20} Nm. The 2013 Mw 6.6 Lushan earthquake has released only a small part ($\sim 1/30$) of the accumulated elastic strain. The seismic moment deficit along the southern LMSF could be capable of generating an Mw 7.6 earthquake, so the seismic hazard there remains high, especially on the unruptured segment further southwest of the 2013 Mw 6.6 Lushan earthquake.

5. Conclusions

We introduce a block modeling approach constrained by horizontal GPS velocities before and after the 2008 Mw 7.9 Wenchuan earthquake to invert the fault coupling along the LMSF, to investigate the relationship between the 2008 Mw 7.9 Wenchuan earthquake and the 2013 Mw 6.6 Lushan earthquake. Our results show the fault coupling dramatically changed along the central and northern LMSF, with fault segments strongly coupled and locked at a depth of ~18 km before the 2008 Mw 7.9 Wenchuan earthquake and decoupled after the earthquake. The seismic gap between the two earthquake rupture zones is coupled within a 5 km depth before the earthquake, and decoupled after the earthquake. Segments along the southern LMSF, including regions around the hypocenter of the 2013 Mw 6.6 Lushan earthquake, however, are coupled from a depth of ~10 km to ~25 km. Moreover, by investigating the GPS velocity changes before and after the 2008 Mw 7.9 Wenchuan earthquake, we find that the postseismic deformation induced by the 2008 Mw 7.9 Wenchuan earthquake has caused the upper crust of Eastern Tibetan Plateau to thrust in an accelerating pace to the Sichuan block, which results in enhanced compression and shear stress on the LMSF. Consequently, downdip coupling of the fault, as well as the accelerating accumulation of the elastic strain, triggered the 2013 Mw 6.6 Lushan earthquake. Additionally, we quantitatively investigate the seismic moment accumulation and release along the southern LMSF. We propose that the 2013 Mw 6.6 Lushan earthquake should be regarded as a “delayed” aftershock of the 2008 Mw 7.9 Wenchuan earthquake. Finally, we suggest that the seismic hazard potential along the southern LMSF remains high, especially on the unruptured segment further southwest of the 2013 Mw 6.6 Lushan earthquake.

Supplementary Materials: The following are available online at <http://www.mdpi.com/2072-4292/10/5/753/s1>, Figure S1, Statistics of the residuals for GPS sites and time series. Figure S2, The block model and GPS velocity residuals. Figure S3, The geometry of the LMSF of our model. Figure S4, Resolution test for fault coupling modeling of the LMSF.

Author Contributions: Y.L. designed and conducted the experiment, processed the GPS data, summarized the research results, and wrote the manuscript; X.S. conducted the project, designed the experiment and summarized the research results; G.Z. summarized the research results and revised the draft; Y.L., C.Q. and X.S. provide insightful comments and suggestions about the interpretation of the 2008 Mw 7.9 Wenchuan earthquake and the 2013 Mw 6.6 Lushan earthquake; Y.W. and H.L. helped to process the GPS data. All authors have read the final manuscript.

Acknowledgments: The authors thank the five anonymous reviewers for their helpful comments and suggestions. Thanks for all of the colleagues who were involved in the GPS data collection. We are grateful to the Sichuan Earthquake Bureau for providing part of the GPS data. We also thank Robert McCaffrey, who has made his block model code (the *TDEFNODE* package) publicly available. This work was funded by the National Natural Science Foundation of China (no. 41631073), the scientific research project of the M 7.0 Jiuzhaigou, Sichuan earthquake, the Basic Scientific Funding of Institute of Geology, China Earthquake Administration (no. IGCEA1613) and the National Key Laboratory of Earthquake Dynamics (LED2015A03). Figures are generated by GMT software [51].

Conflicts of Interest: The authors declare no conflict of interest.

References

1. Burchfiel, B.; Royden, L.; vander Hilst, R.; Hager, B.; Chen, Z.; King, R.; Li, C.; Lü, J.; Yao, H.; Kirby, E. A geological and geophysical context for the Wenchuan earthquake of 12 May 2008, Sichuan, People’s Republic of China. *GSA Today* **2008**, *18*, 4–11. [[CrossRef](#)]
2. Xu, X.; Wen, X.; Yu, G.; Chen, G.; Klinger, Y.; Hubbard, J.; Shaw, J. Coseismic reverse- and oblique-slip surface faulting generated by the 2008 Mw 7.9 Wenchuan earthquake, China. *Geology* **2009**, *37*, 515–518. [[CrossRef](#)]
3. Royden, L.; Burchfiel, B.; King, R.; Wang, E.; Chen, L.; Shen, F.; Liu, P. Surface deformation and lower crustal flow in eastern Tibet. *Science* **1997**, *276*, 788–790. [[CrossRef](#)] [[PubMed](#)]
4. Tapponnier, P.; Xu, Z.; Roger, F.; Meyer, B.; Arnaud, N.; Wittlinger, G.; Yang, J. Oblique stepwise rise and growth of the Tibet Plateau. *Science* **2001**, *294*, 1671–1677. [[CrossRef](#)] [[PubMed](#)]

5. Liu-Zeng, J.; Zhang, Z.; Wen, L.; Tapponnier, P.; Sun, J.; Xing, X.; Hu, G.; Xu, Q.; Zeng, L.; Ding, L.; et al. Co-seismic ruptures of the 12 May 2008, Ms 8.0 Wenchuan earthquake, Sichuan: East-west crustal shortening on oblique, parallel thrusts along the eastern edge of Tibet. *Earth Planet. Sci. Lett.* **2009**, *286*, 355–370. [[CrossRef](#)]
6. Shen, Z.-K.; Sun, J.; Zhang, P.; Wan, Y.; Wang, M.; Bürgmann, R.; Zeng, Y.; Gan, W.; Liao, H.; Wang, Q. Slip maxima at fault junctions and rupturing of barriers during the 12 May 2008 Wenchuan earthquake. *Nat. Geosci.* **2009**, *2*, 718–724. [[CrossRef](#)]
7. Wang, Q.; Qiao, X.; Lan, Q.; Freymueller, J.; Yang, S.; Xu, C.; Yang, Y.; You, X.; Tan, K.; Chen, G. Rupture of deep faults in the 2008 Wenchuan earthquake and uplift of the Longmen Shan. *Nat. Geosci.* **2001**, *4*, 634–640.
8. Jiang, J.; Fialko, Y. Reconciling seismicity and geodetic locking depths on the Anza section of the San Jacinto fault. *Geophys. Res. Lett.* **2016**, *43*, 10663–10671. [[CrossRef](#)]
9. Zhang, P.; Wen, X.; Shen, Z.-K.; Chen, J. Oblique high-angle listric-reverse faulting and associated straining processes: The Wenchuan earthquake of 12 May 2008, Sichuan, China. *Annu. Rev. Earth Planet. Sci.* **2010**, *38*, 353–382. [[CrossRef](#)]
10. Zhang, G.; Vallée, M.; Shan, X.; Delouis, B. Evidence of sudden rupture of a large asperity during the 2008 Mw 7.9 Wenchuan earthquake based on strong motion analysis. *Geophys. Res. Lett.* **2012**, *39*, L17303. [[CrossRef](#)]
11. Huang, Y.; Wu, J.; Zhang, T.; Zhang, D. Relocation of the M8.0 Wenchuan earthquake and its aftershock sequence. *Sci. China Ser. D* **2008**, *51*, 1703–1711. [[CrossRef](#)]
12. Chen, Y.; Yang, Z.; Zhang, Y.; Liu, C. From 2008 Wenchuan earthquake to 2013 Lushan earthquake. *Sci. Sin. Terrae* **2013**, *43*, 1064–1072. (In Chinese)
13. Dong, S.; Han, Z.; An, Y. Paleoseismological events in the “seismic gap” between the 2008 Wenchuan and the 2013 Lushan earthquakes and implications for future seismic potential. *J. Asian Earth Sci.* **2017**, *135*, 1–15. [[CrossRef](#)]
14. Liu, M.; Luo, G.; Wang, H. The 2013 Lushan earthquake in China tests hazard assessments. *Seismol. Res. Lett.* **2014**, *85*, 40–43. [[CrossRef](#)]
15. Liu, C.; Zhu, B.; Yang, X.; Shi, Y. Crustal rheology control on earthquake activity across the eastern margin of the Tibetan Plateau: Insights from numerical modelling. *J. Asian Earth Sci.* **2015**, *100*, 20–30. [[CrossRef](#)]
16. Li, Z.; Tian, B.; Liu, S.; Yang, J. Asperity of the 2013 Lushan earthquake in the eastern margin of Tibetan plateau from seismic tomography and aftershock relocation. *Geophys. J. Int.* **2013**, *195*, 2016–2022. [[CrossRef](#)]
17. Xu, X.; Wen, X.; Han, Z.; Chen, G.; Li, C.; Zheng, W.; Zhang, S.; Ren, Z.; Xu, C.; Tan, X.; et al. Lushan Ms7.0 earthquake: A blind reverse-fault event. *Chin. Sci. Bull.* **2013**, *58*, 3437–3443. [[CrossRef](#)]
18. Wang, Y.; Wang, F.; Wang, M.; Shen, Z.-K.; Wan, Y. Coulomb stress change and evolution induced by the 2008 Wenchuan earthquake and its delayed triggering of the 2013 Mw 6.6 Lushan earthquake. *Seismol. Res. Lett.* **2014**, *85*, 52–59. [[CrossRef](#)]
19. Zhu, S. Is the 2013 Lushan earthquake (Mw = 6.6) a strong aftershock of the 2008 Wenchuan, China mainshock (Mw = 7.9)? *J. Geodyn.* **2016**, *99*, 16–26. [[CrossRef](#)]
20. Li, Y.; Jia, D.; Wang, M.; Shaw, J.; He, J.; Lin, A.; Xiong, L.; Rao, G. Structural geometry of the source region for the 2013 Mw 6.6 Lushan earthquake: implication for earthquake hazard assessment along the Longmen Shan. *Earth Planet. Sci. Lett.* **2014**, *390*, 275–286. [[CrossRef](#)]
21. Parsons, T.; Ji, C.; Kirby, E. Stress changes from the 2008 Wenchuan earthquake and increased hazard in the Sichuan basin. *Nature* **2008**, *454*, 509–510. [[CrossRef](#)] [[PubMed](#)]
22. Toda, S.; Stein, R.; Richards-Dinger, K.; Bozkurt, S. Forecasting the evolution of seismicity in southern California: Animations built on earthquake stress transfer. *J. Geophys. Res.* **2005**, *110*, B05S16. [[CrossRef](#)]
23. Rui, X.; Stamps, D. Present-day kinematics of the eastern Tibetan Plateau and Sichuan Basin: Implications for lower crustal rheology. *J. Geophys. Res.* **2016**, *121*, 3846–3866. [[CrossRef](#)]
24. Herring, T.; King, R.; McClusky, S. *Documentation of the MIT GPS Analysis Software: GAMIT Release 10.4*; Massachusetts Institute of Technology: Cambridge, MA, USA, 2010.
25. Herring, T.; King, R.; McClusky, S. *GLOBK: Global Kalman Filter VLBI and GPS Analysis Program, Release 10.4*; Massachusetts Institute of Technology: Cambridge, MA, USA, 2010.
26. Altamimi, Z.; Métivier, L.; Collilieux, X. ITRF2008 plate motion model. *J. Geophys. Res.* **2012**, *117*, B07402. [[CrossRef](#)]

27. Melnick, D.; Moreno, M.; Quinteros, J.; Baez, J.; Deng, Z.; Li, S.; Oncken, O. The super-interseismic phase of the megathrust earthquake cycle in Chile. *Geophys. Res. Lett.* **2017**, *44*, 784–791. [[CrossRef](#)]
28. Li, Y.; Song, X.; Shan, X.; Qu, C.; Wang, Z. Locking degree and slip rate deficit distribution on MHT fault before 2015 Nepal Mw 7.9 earthquake. *J. Asian Earth Sci.* **2016**, *119*, 78–86. [[CrossRef](#)]
29. Savage, J. A dislocation model of strain accumulation and release at a subduction zone. *J. Geophys. Res.* **1983**, *88*, 4984–4996. [[CrossRef](#)]
30. McCaffrey, R. Time-dependent inversion of three-component continuous GPS for steady and transient sources in northern Cascadia. *Geophys. Res. Lett.* **2009**, *36*, L07304. [[CrossRef](#)]
31. Li, Y.; Shan, X.; Qu, C.; Zhang, Y.; Song, X.; Jiang, Y.; Zhang, G.; Nocquet, J.; Gong, W.; Gan, W.; Wang, C. Elastic block and strain modeling of GPS data around the Haiyuan-Liupanshan fault, northeastern Tibetan Plateau. *J. Asian Earth Sci.* **2017**, *150*, 87–97. [[CrossRef](#)]
32. Wallace, L.; Beavan, J.; McCaffrey, R.; Darby, D. Subduction zone coupling and tectonic block rotations in the North Island, New Zealand. *J. Geophys. Res.* **2004**, *109*, B12406. [[CrossRef](#)]
33. Liu, Q.; Van Der Hilst, R.; Li, Y.; Yao, H.; Chen, J.; Guo, B.; Qi, S.; Wang, J.; Huang, H.; Li, S. Eastward expansion of the Tibetan Plateau by crustal flow and strain partitioning across faults. *Nat. Geosci.* **2014**, *7*, 361–365. [[CrossRef](#)]
34. Huang, M.; Bürgmann, R.; Freed, A. Probing the lithospheric rheology across the eastern margin of the Tibetan Plateau. *Earth Planet. Sci. Lett.* **2014**, *396*, 88–96. [[CrossRef](#)]
35. Wang, Y.; Wang, M.; Shen, Z.-K. Block-like versus distributed crustal deformation around the northeastern Tibetan plateau. *J. Asian Earth Sci.* **2017**, *140*, 31–47. [[CrossRef](#)]
36. Jiang, Z.; Wang, M.; Wang, Y.; Wu, Y.; Che, S.; Shen, Z.-K.; Bürgmann, R.; Sun, J.; Yang, Y.; Liao, H.; Li, Q. GPS constrained coseismic source and slip distribution of the 2013 Mw 6.6 Lushan, China, earthquake and its tectonic implications. *Geophys. Res. Lett.* **2014**, *41*, 407–413. [[CrossRef](#)]
37. Liu, Y.; Wang, C.; Shan, X.; Zhang, G.; Qu, C. Result of SAR differential interferometry for the co-seismic deformation and source parameter of the Ms7.0 Lushan Earthquake. *Chin. J. Geophys.* **2014**, *57*, 2495–2506.
38. Zhang, G.; Hetland, E.; Shan, X.; Vallée, M.; Liu, Y.; Zhang, Y.; Qu, C. Triggered slip on a back reverse fault in the Mw 6.8 2013 Lushan, China earthquake revealed by joint inversion of local strong motion accelerograms and geodetic measurements. *Tectonophysics* **2016**, *672*, 24–33. [[CrossRef](#)]
39. Zhao, J.; Jiang, Z.; Wu, Y. Study on fault locking and fault slip deficit of the Longmenshan fault zone before the Wenchuan earthquake. *Chin. J. Geophys.* **2012**, *55*, 2963–2972.
40. Zhao, J.; Wu, Y.; Jiang, Z. Fault locking and dynamic deformation of the Longmenshan fault zone before the 2013 Lushan Ms 7.0 earthquake. *Acta Seismol. Sin.* **2013**, *35*, 681–691.
41. Wu, Y.; Jiang, Z.; Wang, M. Preliminary results of the co-seismic displacement and pre-seismic strain accumulation of the Lushan Ms7.0 earthquake reflected by the GPS surveying. *Chin. Sci. Bull.* **2013**, *58*, 1910–1916. [[CrossRef](#)]
42. Xiao, Z.; Xu, C.; Jiang, G. Crustal strain in the Longmenshan region considering fault locking during ten years before the 2008 Wenchuan earthquake. *Chin. J. Geophys.* **2017**, *60*, 953–961.
43. Ran, Y.; Chen, W.; Xu, X.; Chen, L.; Wang, H.; Yang, C.; Dong, S. Paleoseismic events and recurrence interval along the Beichuan-Yingxiu fault of Longmenshan fault zone, Yingxiu, Sichuan, China. *Tectonophysics* **2013**, *584*, 81–90. [[CrossRef](#)]
44. Zhang, Y.; Feng, P.; Xu, L.; Zhou, C.; Chen, Y. Spatio-temporal rupture process of the 2008 great Wenchuan earthquake. *Sci. China Ser. D* **2009**, *52*, 145–154. [[CrossRef](#)]
45. Xu, Y.; Li, Z.; Huang, R.; Xu, Y. Seismic structure of the Longmen Shan region from S-wave tomography and its relationship with the Wenchuan Ms 8.0 earthquake on 12 May 2008, southwestern China. *Geophys. Res. Lett.* **2010**, *37*, 211–228. [[CrossRef](#)]
46. Wang, Z.; Su, J.; Liu, C.; Cai, X. New insights into the generation of the 2013 Lushan earthquake (Ms7.0), China. *J. Geophys. Res.* **2015**, *120*, 3507–3526. [[CrossRef](#)]
47. Zhu, S.; Yuan, J. Mechanisms for the fault rupture of the 2008 Wenchuan earthquake (Ms = 8.0) with predominately unilateral propagation. *Chin. J. Geophys.* **2016**, *59*, 4063–4074.
48. Duan, B. Role of initial stress rotations in rupture dynamics and ground motion: A case study with implications for the Wenchuan earthquake. *J. Geophys. Res.* **2010**, *115*, B05301. [[CrossRef](#)]
49. Scholz, C. *The Mechanics of Earthquakes and Faulting*; Cambridge University Press: Cambridge, UK, 2002; 225p.

50. Savage, J.; Prescott, W. Asthenosphere readjustment and the earthquake cycle. *J. Geophys. Res.* **1978**, *83*, 3369–3376. [[CrossRef](#)]
51. Wessel, P.; Smith, W.; Scharroo, R.; Luis, J.; Wobbe, F. Generic mapping tools: Improved version released. *Eos Trans. AGU* **2013**, *94*, 409–410. [[CrossRef](#)]



© 2018 by the authors. Licensee MDPI, Basel, Switzerland. This article is an open access article distributed under the terms and conditions of the Creative Commons Attribution (CC BY) license (<http://creativecommons.org/licenses/by/4.0/>).